Constrained optimal control: an application to semiactive suspension systems

Tina Paschedag
Institute of Automatic Control Engineering (LSR), Technische Universitaet Muenchen
D-80290 Munich, Germany
Tel: +49-89-289-23404, Fax: +49-89-289-28340, tina.paschedag@tum.de.

Alessandro Giua*, Carla Seatzu
Dept. of Electrical and Electronic Eng., University of Cagliari
Piazza d'Armi — 09134 Cagliari, Italy
Tel: +39-070-675-5759, Fax: +39-070-675-5782, {giua,seatzu}@diee.unica.it.

Abstract

This paper applies three different control techniques to the design of a quarter car semiactive suspension system. The three techniques, originally developed to solve a constrained optimal control problem, are *optimal gain switching*, *discontinuous variable structure control* and *explicit model predictive control*. All of them divide the state space into convex regions and assign a linear or affine state feedback controller to each region. The partition of the state space is computed off-line. During the on-line phase, the controller switches between the subcontrollers according to the current state. All the above techniques gave satisfactory results when applied to the design of semiactive suspension systems. A detailed comparison in terms of computational complexity, performance and simplicity of the design is proposed in the paper.

Published as:
T. Paschedag, A. Giua, C. Seatzu, Constrained optimal control: an application to semiactive suspension systems, *Int. Journal of Systems Science*, Vol. 41, No. 7, pp. 797-811, July 2010.

*Contact author to whom all correspondence should be addressed.

1 Introduction

The design of active suspensions for road vehicles aims to optimize the performance of the vehicle with regard to comfort, road holding and rideability [13, 25]. In an active suspension the interaction between vehicle body, the so-called sprung mass, and wheel (nonsprung mass) is regulated by an actuator of variable length. The actuator is usually hydraulically controlled and applies between body and wheel a force that represents the control action generally determined with an optimization procedure.

In contrast to active suspensions, passive suspensions consist of dampers and springs and the interaction between body and wheel is determined by their elastic constants and damping coefficients, that are constant.

A good tradeoff between active and passive suspensions in terms of performance and costs is given by semiactive suspensions [9, 19, 23]. A semiactive suspension system consists of a spring and a damper: the spring has a constant stiffness, while the damper has a characteristic coefficient f that can be modified within an interval $[f_{\min}, f_{\max}]$. In particular, the active suspension system may be assumed as a target, and at any time instant, the value of f is chosen so as to make the evolution of the semiactive suspension system as close as possible to that of the active suspension.

The main objective of this paper is that of discussing the applicability of some optimal control methods to the design of a semiactive suspension system. In particular, we consider three different techniques to control linear systems with state or input constraints and, assuming the semiactive suspension system as a case study, we compare them under several aspects, namely range of applicability, computational complexity and performance. In particular, the considered approaches are *explicit model predictive control* (eMPC) [3, 7], *optimal gain switching* (OGS) [27], and *discontinuous variable structure control* (dVSC) [1, 2, 17].

As well known, the two most commonly used approaches to optimally control *linear systems with state or input constraints* are based on *anti-windup* and *model predictive control*.

- Anti-windup schemes are auxiliary to control schemes that are able to provide efficient performance around nominal operating conditions. Their goal is that of preventing the violation of certain constraints (windup phenomenon) using a control scheme that does not modify the behavior of the original controller if saturation does not occur, while it becomes active when certain bounds are exceeded. The most popular synthesis tools for the design of anti-windup compensators are based on linear matrix inequalities (LMI). However, even if several works have been presented in this framework [4, 18, 24, 28], a systematic approach for the synthesis of anti-windup schemes that guarantee closed-loop stability and optimal performance is still missing. In particular, this is the case when dealing with complex constrained multivariable control problems.

- The *implicit* model predictive control approach is based on the solution of an optimal control problem at each sampling time, starting from the current state. The optimal control problem is solved over a given time horizon that may either be finite or infinite. At the next time step the optimization is repeated considering an horizon of the same length of the previous one, but shifted. This is the reason why such an approach is also known as *moving horizon control*. The main drawback is that it requires the solution of an optimization problem at each sampling time, whose complexity may be prohibitive for large horizons and in the case of high sampling frequency.

An alternative to the classical implicit model predictive control has recently been proposed by Bemporad *et al.* [3, 7]: this new approach is called *explicit model predictive control* (eMPC). Its main advantage is that the most burdensome part of the procedure is moved off-line. By appropriately converting the optimal control problem with constraints into a multi-parametric programming problem, appropriate algorithms in this framework can be used, and the state space is partitioned into polytopes described by linear inequalities[1]. A piecewise affine control law is associated to each region, thus the on-line phase of the procedure simply consists in determining the current region and assigning accordingly the appropriate control law.

There exist two other interesting approaches that share the same philosophy of eMPC, namely that of solving the optimal control problem for constrained linear systems with a procedure that requires both an off-line and an on-line phase. During the off-line phase the state space is partitioned into a finite number of convex regions and to each region a linear subcontroller is assigned. During the on-line phase the controller switches between these subcontrollers according to the current system state. These approaches are called *optimal gain switching* (OGS) [27], and *discontinuous variable structure control* (dVSC) [1, 2, 17].

All three approaches, i.e., OGS, dVSC and eMPC, guarantee closed-loop stability. However, eMPC is the most general in the sense that it can take into account general constraints of the form

$$Ex(t) + Lu(t) \leq M \tag{1}$$

where $x(t) \in \mathbb{R}^n$ is the state, $u(t) \in \mathbb{R}^m$ is the control input, and E, L and M are matrices of suitable dimension. On the contrary, the other two approaches can only deal with *symmetric* constraints of the form

$$|u(t) - k^T x(t)| \leq u_{max} \tag{2}$$

where $u(t) \in \mathbb{R}$ is a scalar input and $k \in \mathbb{R}^n$ is a constant gain vector. Constraints (2) are obviously a particular case of (1).

The OGS procedure has been successfully applied in [12] to the design of quarter-car suspension systems, where the constraint on the input takes the form $|u(t)| \leq u_{\max}$, i.e., is a special case of (2). The procedure is used for the design of *active* control laws, that can be approximated

[1] A bounded polyhedron $\mathcal{P} \subset \mathbb{R}^n$, $\mathcal{P} = \{\boldsymbol{x} \in \mathbb{R}^n \mid \boldsymbol{A}\boldsymbol{x} \leq \boldsymbol{B}\}$ is called a *polytope*.

using a *semiactive* suspension system. In this paper we investigate if dVSC and eMPC can also be applied to semiactive suspension design.

1.1 Relevant literature on semiactive suspensions

Several newly designed top cars already use semiactive suspension systems. As a result great efforts are now devoted to improve their efficiency, as demonstrated by the large number of publications in this area.

A comprehensive survey on this topic is given in [14]. Here the author surveys applications of optimal control techniques (basically focusing on linear quadratic optimal control) to the design of active and semiactive suspensions, starting from the quarter-car model, but also considering the half-car and the full-car models. Another more recent survey is given in [15] by Jalili.

In [6] the authors present a learning algorithm using neural networks which allows a vehicle with semi-active suspension to improve continuously not only the ride comfort but also the tyre/ground contact.

In [8] Canale, Milanese and Novara propose a solution that is based on MPC. In particular, they try to overcome the problems typically related to the online implementation of MPC strategies using a "fast" MPC implementation based on nonlinear function approximation techniques. The proposed solution is also successfully compared with well-established control algorithms such as "two state" Sky-Hook [14] and "clipped" strategy [21].

Giorgetti et al. in [10] modeled the constrained quarter-car semiactive suspension as a switching affine system, where the switching is determined by the activation of passivity constraints, force saturation, and maximum power dissipation limits. Explicit optimal control laws have been derived with different finite horizons, and it has been shown that the optimal control is piecewise affine in state.

Finally, the use of magnethoreological dampers has been considered in [11, 16].

1.2 Structure of the paper

The paper is structured as follows. In Sections 2 and 3 we provide some background on the OGS and the VSC procedure, respectively. In Section 4 we recall the main features of the eMPC approach and the main design parameters necessary to implement it using the MATLAB Multi-Parametric Toolbox [20]. In Section 5 we present the linear dynamical models of the suspension system considered in the paper. A comparison among the three considered approaches when applied to the design of suspension systems is given in Section 6. Conclusions are finally drawn in Section 7.

2 Optimal gain switching

Let us consider a linear and time-invariant system

$$x(t+1) = Gx(t) + Hu(t), \tag{3}$$

where $t \in \mathbb{N} = \{0, 1, 2, \ldots\}$, $x \in \mathbb{R}^n$, $u \in \mathbb{R}$.

We want to determine the control law $u^*(\cdot)$ that minimizes a performance index of the form:

$$J = \sum_{t=0}^{\infty} x^T(t) Q\, x(t), \tag{4}$$

(with Q positive semidefinite) under the constraint

$$|u(t)| \leq u_{max} \quad (t \geq 0). \tag{5}$$

It is well known that the optimal solution $u^*(\cdot)$ does not correspond to a feedback control law [26].

The OGS approach, firstly proposed by Yoshida in [27], approximates the optimal control law $u^*(\cdot)$ by switching among a certain number of feedback control laws whose gains can be computed as the solution of a family of LQR problems. More precisely, to determine the OGS control law u_{OGS} we consider a family of performance indices

$$J_\rho = \sum_{t=0}^{\infty} [\, \rho\, x^T(t) Q\, x(t) + u^T(t) R u(t)], \quad \rho > 0,\ R > 0. \tag{6}$$

For a given value of ρ, the unconstrained control law that minimizes J_ρ can be written as

$$u_\rho(t) = -k_\rho^T\, x(t) \tag{7}$$

where the gain vector k_ρ^T is obtained by solving an algebraic Riccati equation. The resulting controller then switches among different control laws in the form (7) depending on the current value of the system state.

For a given value of ρ it is possible to compute a *linear region* Γ_ρ in the state space such that for any point x_0 within this region the following equation holds:

$$|u_\rho(t)| \equiv |k_\rho^T (G - H k_\rho^T)^t\, x_0| \leq u_{max}, \quad (t \geq 0). \tag{8}$$

Thus, considering the system (3) controlled with u_ρ and an initial state $x_0 \in \Gamma_\rho$, we can be sure that in its future evolution the value of the control input will always satisfy the constraint (5).

A finite set of m values of ρ, namely $\{\rho_1, \ldots, \rho_m\}$ should be first selected. A good choice of the ρ_i's may influence the performance of the OGS law. As m increases, the performance index J_ρ decreases, but the procedure becomes computationally more intensive. The weighting coefficient

ρ_1 should be determined such that the linear region Γ_{ρ_1} contains all the initial conditions of interest. The weighting coefficient ρ_m should be selected such that the region Γ_{ρ_m} covers small disturbances or very small system noises. The coefficients $\rho_2, \ldots, \rho_{m-1}$ should be chosen taking into account the size of the linear region Γ_i. Once ρ_1, ρ_m and m are determined, the intermediate values of ρ can be chosen such that the ratios of the norm between two adjacent gains are constant, i.e.,

$$\frac{||k_{\rho_i}||}{||k_{\rho_{i-1}}||} = \left(\frac{||k_{\rho_m}||}{||k_{\rho_1}||}\right)^{\frac{1}{m}}. \tag{9}$$

Then, following a simple procedure given in [27], the regions Γ_ρ's are computed off-line. Such a procedure, that is not reported here for brevity's requirements, is based on the solution of m linear programming problems that provide appropriate vectors z_ρ's. At each sampling time t the on-line phase of the approach simply requires to determine the largest value v such that

$$v = \max\{\, i \mid x(t) \in \Gamma_{\rho_i},\ i = 0, \ldots, m\} \tag{10}$$

and set $\rho(t) = \rho_v$. The condition $x(t) \in \Gamma_\rho$ is true iff

$$-u_{\max} \leq z_\rho^T x_0 \leq u_{\max} \tag{11}$$

where $z_\rho^T = k_\rho^T(G - Hk_\rho^T)$. Thus the control law at time t is chosen equal to

$$u_{\mathrm{OGS}}(t) = -k_{\rho_v}^T x(t). \tag{12}$$

It has been shown by Yoshida that if no disturbance is acting on the system, $\rho(t)$ is a nondecreasing function of t.

3 Discontinuous Variable Structure Control

The basic ideas of discontinuous VSC (dVSC) have been firstly proposed by Kiendl and Schneider [17]. Most of the literature on this topic is in German, but a good survey in English is available [2].

The variable structure controller, depending on the system's state, either switches between a finite number of linear subcontrollers (discontinuous VSC) or changes the controller parameters continuously (soft VSC) with the objective of obtaining a better performance in terms of shorter settling times while avoiding violation of control signal constraints.

The dVSC method makes use of a set of nested, positively invariant sets each with a dedicated linear controller. During the regulation cycle, the trajectory runs from a positively invariant region in the state space into the next smaller one, simultaneously activating the assigned controller.

Here we briefly outline the general structure of the dVSC.

Consider the linear time-invariant plant in continuous time

$$\dot{x}(t) = Ax(t) + Bu(t) \tag{13}$$

where $t \in \mathbb{R}_{\geq 0}$, $x \in \mathbb{R}^n$, $u \in \mathbb{R}$, under the control signal constraint

$$|u(t)| \leq u_{\max}. \tag{14}$$

The control input is chosen according to

$$u_{dVSC}(t) = \mathcal{F}(x(t), p) \tag{15}$$

where $\mathcal{F}$ is an operator[2] that depends on the system's state x and a selection parameter p, that is computed by a selection strategy or supervisor, i.e., $p = S(x)$, defined by a discontinuous function S. The selection strategy switches between a finite number m of different subcontrollers so as to optimize the system's performance in terms of *settling times*.

Note that in the following we consider only bounded sets $X_0 \subset \mathbb{R}^n$ of possible initial vectors $x(t = 0)$, since $X_0 = \mathbb{R}^n$ is usually not of practical interest. The three major steps of the dVSC design procedure are:

(D1) Choose a family of m linear state controllers $u(t) = -k_p^T\, x(t)$ leading to stable control loops

$$\dot{x}(t) = (A - Bk_p^T)\, x(t) = \hat{A}_p\, x(t), \quad p = 1, \ldots, m \tag{16}$$

whose response times decrease with increasing index p.

(D2) According to each control loop (16) construct a Lyapunov region

$$G_p = \{x \mid v_p(x) < c_p\} \tag{17}$$

where c_p determines the size of G_p. Moreover, G_p should be such that all $x \in G_p$ satisfy the constraint $|u_{dVSC}| = |k_p^T\, x| \leq u_{\max}$.

(D3) The Lyapunov regions should be nested one inside the other in accordance with

$$G_{p+1} \subset G_p, \quad p = 1, \ldots, m-1 \tag{18}$$

with an increasing index p.

The dVSC method follows an approach similar to the OGS design, and consists of an off-line and an on-line phase. The three steps mentioned above represent the off-line phase. During the on-line phase the controller determines the smallest Lyapunov region that contains the current

[2] A common practice, as we do in this section, is that of choosing $u_{dVSC}(t) = -k_p^T x(t)$.

system's state and activates the subcontroller corresponding to this region. As soon as the trajectory enters a smaller region, the controller switches to the corresponding subcontroller.

In the first step the subcontrollers' vectors k_p are determined utilizing *pole placement* such that the n eigenvalues $\lambda_{p,j}$ of $\hat{A}_p$ conform to

$$\lambda_{p+1,j} = h\,\lambda_{p,j}, \quad h > 1 \tag{19}$$

and lead to a stable closed loop, i.e. $Re\{\lambda_p\} < 0$. These controllers thus accelerate the control system's behavior, while simultaneously causing a similar behavior, since the eigenvalue configuration remains the same.

In a second step the Lyapunov regions are constructed employing quadratic Lyapunov functions $v_p(x) = x^T R_p\,x$, where the matrix R_p is the solution of the Lyapunov equation $\hat{A}_p^T R_p + R_p\,\hat{A}_p = -Q_p$.

The matrices Q_p have to be positive-definite: $Q_{p+1} = Q_p$ is frequently a reasonable choice. Thus, the Lyapunov regions will be ellipses determined by the matrices R_p. Since the condition $|k_p^T\,x| \leq u_{\max}$ has to be satisfied for all $x \in G_p$, to ensure the regions G_p are as large as possible the constant c_p in (17) are chosen such that the hyperplanes $\pm k_p^T\,x = u_{\max}$ are tangent to the elliptical Lyapunov regions. A suitable c_p is

$$c_p = \frac{u_{\max}^2}{k_p^T\,R_p^{-1} k_p}. \tag{20}$$

and it can be determined solving a quadratic optimization problem [2].

The largest Lyapunov region G_1 has to be determined such that $X_0 \subseteq G_1$, i.e. the first region includes all possible initial states.

Finally, in a third step we verify that all regions G_p's are nested: if all points of interest satisfy

$$\frac{x^T R_p\,x}{c_p} < \frac{x^T R_{p+1}\,x}{c_{p+1}} < 1 \tag{21}$$

then $G_{p+1} \subset G_p$ is ensured. To check whether (21) is true or not it is sufficient to make sure that the matrices

$$\frac{R_{p+1}}{c_{p+1}} - \frac{R_p}{c_p} \tag{22}$$

are positive definite for $p = 1, \ldots, m-1$.

We conclude pointing out that the most burdensome step in this design procedure is the determination of a suitable matrix R_1 (from which all other matrices R_p for $p > 1$ can also be derived). Several techniques to do this, based on nonlinear optimization, have been presented in the literature [1, 2].

4 Explicit model predictive control

Model Predictive Control (MPC) [5], also referred as *moving horizon control* or *receding horizon control*, is an advanced control method that has become an attractive feedback strategy, especially for linear and time-invariant systems of the form (3) under the constraint (5), that are those of interest here.

The basic idea of MPC is the following: at every time step, the control action is chosen solving an optimal control problem, minimizing a performance criterion over a future horizon. Only the first control command will be applied and after one time step other measurements will be got and the optimization problem is repeated. This is an on-line procedure and in many cases it is difficult (or even impossible) to implement because the on-line solution of a linear or quadratic program, depending on the performance index, is required. Various MPC algorithms use different cost functions to obtain the control action. In this paper we consider the following standard form:

$$J_N(x(t)) = \sum_{j=0}^{N} x(t+j)^T Q x(t+j) + u(t+j)^T R u(t+j) \tag{23}$$

where Q and R are positive definite matrices.

The main limitation of the implicit MPC is that the computations are executed on-line, so that it is only applicable to relatively slow and/or small problems.

The explicit MPC approach is based on multi-parametric programming. It moves all the burdensome computations off-line and partitions the state space into polytopic regions, so that during the on-line phase of the control procedure according to the current state the actual subcontroller can be found out of a table. The on-line phase of the eMPC is similar to that one of the other approaches presented above (OGS and dVSC).

Algorithms to compute the polytopic regions are given in [3, 7]. Moreover, the eMPC controller can be computed using the Multi-Parametric Toolbox (MPT) [20], a free and user-friendly MATLAB toolbox for design, analysis and deployment of optimal controllers for constrained linear and hybrid systems.

As already pointed out in [3, 7], the main drawback of the eMPC is that it may easily lead to controllers with prohibitive complexity, both in runtime and solution. In particular, there are three aspects which are important in this respect: performance, closed-loop stability and constraint satisfaction. The MPT toolbox provides several possibilities to compute the controller and the partition of the state space, which are specified below and that we have investigated.

— *Finite Time Optimal Control (FTOC).* This method yields the finite time optimal controller, i.e. the performance will be N-step optimal but may not be infinite horizon optimal. The complexity of the controller depends strongly on the prediction horizon N, the larger

N the more complex the controller is. Furthermore, within this method, the MPT toolbox provides two different modes.

- `probstruct:Tconstraint=0:` The controller will be defined over a superset of the maximum controllable set (i.e. all states, which are controllable to the origin), but no guarantees on stability or closed-loop constraint satisfaction can be given. As the prediction horizon N is increased the feasible set of states will converge to the maximum controllable set from "the outside-in", i.e., the controlled set will shrink as N increases[3].
- `probstruct:Tconstraint=1:` The resulting controller will guarantee stability and constraint satisfaction for all time, but will only cover a subset of the maximum controllable set of states. By increasing the prediction horizon, the controllable set of states will converge to the maximum controllable set from "the inside-out", i.e. the controlled set will grow larger as N increases.

— *Infinite Time Optimal Control (ITOC).* This method yields the infinite time optimal controller, i.e. the best possible performance for the control problem. Asymptotic stability and constraint satisfaction are guaranteed and the maximum controllable set will be covered by the resulting controller. However, the controller's complexity may be prohibitive and the computation may take a very long time.

Two other options are possible when designing the eMPC controller using the toolbox MPT, namely *Minimum Time Control* and *Low Complexity Control*. However, we do not discuss these cases here because we have not been able to apply them to our application: in both cases the computation did not finish in adequate times.

5 Dynamical model of the suspension system

In this paper we consider two different dynamical models of a quarter-car suspension system. The first one is a two-degrees of freedom fourth-order model [12]. The second one is a reduced one-degree of freedom second-order model that neglects the dynamics of the tire.

Since the reduced model does not describe the interaction of the tire with the suspended mass and the ground, it cannot be used to evaluate features like road holding and rideability. However, as it will be discussed later, it allows a significant comparison among the different design techniques we considered.

[3]Even though closed loop stability and constraint satisfaction are not guaranteed, MPT provides a function to extract the set of states which satisfy the constraints for all time and another function to analyze these states for stability.

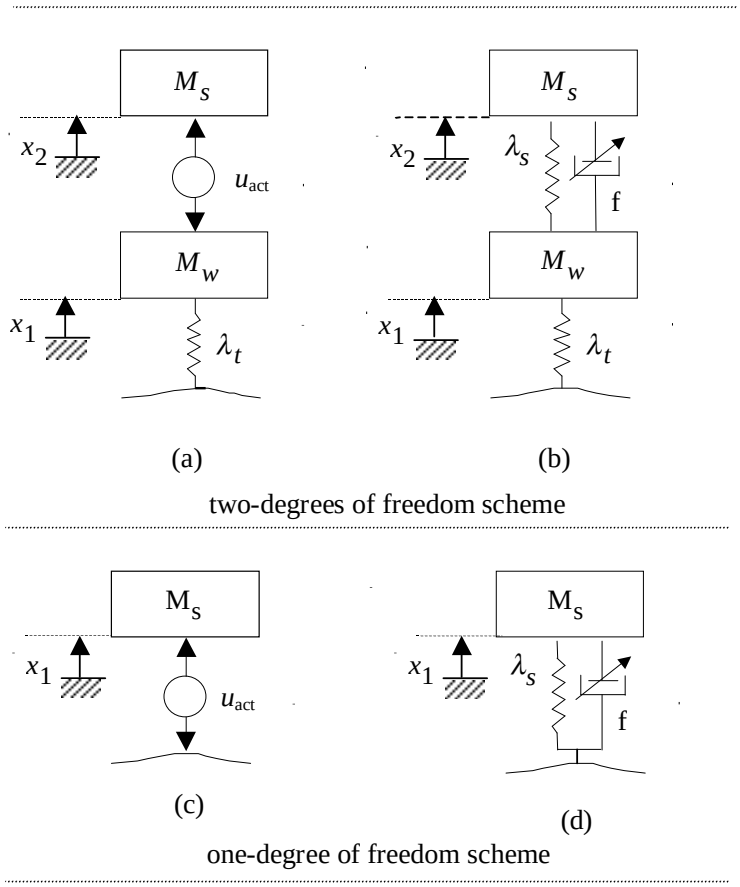

Figure 1: Scheme of the fourth-order suspension model: (a) active; (b) semiactive. Scheme of the second-order suspension model: (c) active; (d) semiactive.

5.1 Fourth-order model

The fourth-order model is depicted in Fig. 1.a (active suspension) and Fig. 1.b (semiactive suspension), where we used the following notation:

- M_w is the nonsprung mass consisting of the wheel and its moving parts;
- M_s is the sprung mass, i.e. the part of the whole body mass and the load mass pertaining to only one wheel;
- $x_1(t)$ is the nonsprung mass displacement at time t with respect to a fixed reference;
- $x_2(t)$ is the sprung mass displacement at time t with respect to a fixed reference;
- $x_3(t) = \dot{x}_1(t)$ is the velocity of the nonsprung mass at time t;
- $x_4(t) = \dot{x}_2(t)$ is the velocity of the sprung mass at time t;

- $u_{\text{act}}(t)$ is the active control force at time t;
- λ_t is the elastic constant of the tire, whose damping characteristics have been neglected. This is in line with almost all researchers who have investigated synthesis of active suspensions for motor vehicles as the tire damping is minimal [11, 12, 25];
- λ_s is the elastic constant of the spring of the semiactive suspension;
- $f(t)$ is the adjustable damper coefficient of the semiactive suspension at time t.

5.1.1 Active suspensions

The state equation of the active suspension system is

$$\dot{x}(t) \quad = \quad A\,x(t) + B\,u(t) \tag{24}$$

where

$$A = \begin{bmatrix} 0 & 0 & 1 & 0 \\ 0 & 0 & 0 & 1 \\ -\frac{\lambda_t}{M_w} & 0 & 0 & 0 \\ 0 & 0 & 0 & 0 \end{bmatrix},\ B = \begin{bmatrix} 0 \\ 0 \\ -\frac{1}{M_w} \\ \frac{1}{M_s} \end{bmatrix}.$$

In such an active suspension system it is required that the control force satisfy a constraint of the form [12]:

$$|u_{\text{act}}(t)| \leq u_{\max}. \tag{25}$$

This constraint bounds the acceleration of the sprung mass – at least in nominal operating conditions, i.e., when the linear model of the suspension is valid – so as to ensure the comfort of the passengers and to avoid loss of contact between wheel and road. Furthermore, this constraint limits the maximal force required from the controller, i.e., it leads to the choice of a suitable actuator.

The control laws all require the knowledge of the system's state x. Since not every component of $x(t)$ is directly measurable, we reconstruct the state through an appropriate state observer. To do this, we choose a suitable output $y(t) = Cx(t)$, with $C = [1\ {-1}\ 0\ 0;\ 0\ 0\ 0\ 1]$, which corresponds to measuring the suspension deformation and the sprung mass velocity. The resulting system is thus observable and controllable[4].

Moreover, as discussed in the following, both the OGS and the eMPC approaches make use of a discrete-time state space model. Therefore, we choose a sampling interval T and discretize the model (24), thus getting the new model

$$x(t+1) = Gx(t) + Hu(t) \tag{26}$$

[4]Note that an observer causes performance loss, notably with respect to the actuator saturation. This problem is not considered here when comparing the three different approaches.

where

$$G = e^{AT}, \qquad H = \left(\int_0^T e^{A\tau} d\tau \right) B. \tag{27}$$

It is well known [22] that a system that is observable and controllable in the absence of sampling maintains these properties after the introduction of sampling if and only if, for every eigenvalue of A for the continuous time control system, the relationship $Re\{\lambda_i\} = Re\{\lambda_j\}$ implies $Im\{\lambda_i - \lambda_j\} \neq \frac{2n\pi}{T}, \quad n = \pm 1, \pm 2, \ldots$. The problem at hand results in the following set of eigenvalues: $\left\{0, 0, \sqrt{-\frac{\lambda_t}{M_w}}, -\sqrt{-\frac{\lambda_t}{M_w}}\right\}$. Under these conditions it is necessary to choose a sampling period T, such that: $T \neq n\pi\sqrt{\frac{M_w}{\lambda_t}}$.

5.1.2 Semiactive suspensions

The effect of the semiactive suspension which is composed of a spring and a damper with an adjustable damper coefficient (see Fig. 1.b) leads to the semiactive control law

$$u_{\text{sem}}(t) = -[-\lambda_s \quad \lambda_s \quad -f(t) \quad f(t)] \cdot x(t).$$

Note that, as f may vary, $u_{\text{sem}}(t)$ is both a function of f and of $x(t)$.

In general, f may only take values in a real set $[f_{\min}, f_{\max}]$. We propose to choose at each step t the value of $f(t)$ to minimize the difference $F[f, x(t)] = (u_{\text{act}}(t) - u_{\text{sem}}(t))^2$. Note that different approaches can be used to derive the active force u_{act} assumed as a target for the semiactive suspension system. Nevertheless, the following rule to update the value of f is applicable in all such cases.

Let us first assume $x_3(t) \neq x_4(t)$, then the value $f^*(t)$ such that $F[f^*(t), x(t)] = 0$ is

$$f^*(t) = -\frac{u_{\text{act}}(t) + \lambda_s \, \Delta\, x(t)}{\Delta\, v(t)} \tag{28}$$

where $\Delta x(t) = x_2(t) - x_1(t)$ is the suspension deformation and $\Delta v(t) = x_4(t) - x_3(t)$ is its rate of change.

As the admissible values of f lie in the interval $[f_{\min}, f_{\max}]$ the adjusted damper coefficient becomes

$$\begin{aligned} f(t) = \quad & \text{minarg}_{f \in [f_{\min}, f_{\max}]} F[f, x(t)] = \\ & \begin{cases} f_{\max} & \text{if} \quad f^*(t) > f_{\max} \\ f^*(t) & \text{if} \quad f^*(t) \in [f_{\min}, f_{\max}] \\ f_{\min} & \text{if} \quad f^*(t) < f_{\min} \end{cases} \end{aligned} \tag{29}$$

When $x_3(t) = x_4(t)$, regardless to the values of f, the damper does not give any contribution to $u_{\text{sem}}(t)$. Thus, in this case we assume $f(t) = f_{\max}$, which we choose also as the initial value for the damper coefficient $f(0) = f_{\max}$.

5.2 Second-order model

The second-order model of the suspension system is shown in Fig. 1.c (active suspension) and Fig. 1.d (semiactive suspension), where we used the following new notation:

- $x_1(t)$ is the sprung mass displacement at time t with respect to a fixed reference;
- $x_2(t) = \dot{x}_1(t)$ is the velocity of the sprung mass at time t.

5.2.1 Active suspensions

The continuous-time state space model of the active suspension is in the form (24) with constraint (25), and

$$A = \begin{bmatrix} 0 & 1 \\ 0 & 0 \end{bmatrix}, \quad B = \begin{bmatrix} 0 \\ 1/M_s \end{bmatrix}.$$

while the discrete-time model can be obtained using eq. (27).

5.2.2 Semiactive suspensions

The effect of the semiactive suspension is equivalent to that of a control force

$$u_{\text{sem}}(t) = -[\lambda_s \quad f(t)]\, x(t).$$

Thus, minimizing $(u_{\text{act}}(t) - u_{\text{sem}}(t))^2$ under the assumption $x_2(t) \neq 0$, results in a damper coefficient

$$f^*(t) = -\frac{u_{\text{act}} - \lambda_s\, x_1(t)}{x_2(t)}. \tag{30}$$

As the damper coefficient has to be chosen out of the set $[f_{\min}, f_{\max}]$, $f(t)$ is determined considering (29).

6 A comparison among the different approaches

In this section we compare the three control design methods above applying them to the suspension system illustrated in Section 5.

Following [12], we take: $M_w = 28.58$ Kg, M_s=288.90 Kg, $\lambda_t = 155900$ N/m, $\lambda_s = 14345$ N/m. We assume the sampling time equal to $T = 0.01$ s, to which it corresponds the sampling frequency $\omega_s = 2\pi/T \simeq 6 \cdot 10^2$ rad/s.

The above choice of ω_s is essentially due to the following reasons. Firstly, the bandwidth of the passive suspension system described by (24) is $\omega_b < 2 \cdot 10^2$ rad/s. A sampling frequency of

$\omega_s \simeq 6 \cdot 10^2$ rad/s is in good agreement with Shannon's theorem [22] that requires $\omega_s > 2\omega_b$. Moreover, this choice of sampling interval ensures that the system will maintain the properties of controllability and observability. Finally, to change f the controller must change the opening of the damper valve. Present technologies impose a limit of about 10^2 Hz on the updating frequency of the damper coefficient.

Moreover, we take $u_{\max} = 3000$ N that is slightly less than the total weight resting on one wheel. Note that this does not prevent loss of contact between wheel and road. Furthermore, this constraint also limits the acceleration of the sprung mass and this is a necessary condition for the comfort of passengers.

Finally we choose $f(t) \in [800, 3000]$ Ns/m.

Other parameters are given in the following.

— *OGS*. When dealing with the fourth-order model we assume $Q = [11 \ -1 \ 0 \ 0; \ -1 \ 1 \ 0 \ 0; \ 0 \ 0 \ 0 \ 0; \ 0 \ 0 \ 0 \ 0]$ and $R = 0.8 \cdot 10^{-9}$, that lead to a good performance in terms of road holding and passenger's comfort. Finally, as in [12] we choose the parameters ρ_i's as follows: $\rho_1 = 0.01$, $\rho_2 = 0.1$, $\rho_3 = 0.5$, $\rho_4 = 1$, $\rho_5 = 4$, $\rho_6 = 20$, $\rho_7 = 50$, $\rho_8 = 100$, $\rho_9 = 1000$, $\rho_{10} = 10^5$. When dealing with the second-order model we assume $Q = [1 \ 0; \ 0 \ 0]$, $R = 0.8 \cdot 10^{-9}$, and $\rho_1 = 0.5$, $\rho_2 = 1$, $\rho_3 = 4$, $\rho_4 = 20$, $\rho_5 = 50$.

— *dVSC*. In the case of the fourth-order model controller we assume that the set of eigenvalues of the first controller ($p = 1$) are placed at

$$\lambda_{1,2} = -4.5893 \pm 73.7067j \qquad \lambda_{3,4} = -2.9243 \pm 2.2560j$$

while the remaining nine (here the total number of regions is $m = 10$) are chosen assuming $h = 1.1$ in (19).

We assumed[5] a matrix R_1 equal to

$$R_1 = \begin{bmatrix} 352.0693 & -1.4000 & 0.0246 & -1.6864 \\ -1.4000 & 11.9693 & -0.0216 & 4.1430 \\ 0.0246 & -0.0216 & 0.0667 & -0.0071 \\ -1.6864 & 4.1430 & -0.0071 & 1.8548 \end{bmatrix}.$$

This enables us to determine matrix $Q_1 = -(A_1^T R_1 + R_1 A_1)$, where $A_1 = A - Bk_1^T$ and k_1 is the feedback controller that imposes the desired set of eigenvalues $\lambda_{1,2}$ and $\lambda_{3,4}$. Finally, assuming $Q_p = Q_1$ and solving $Q_p = -(A_p^T R_p + R_p A_p)$ for all $p = 2, \ldots, 10$ we are also able to determine all other matrices R_p.

[5] In both cases (fourth order and second order model) suitable values for matrix R_1 leading to good performance were provided by an anonymous reviewer.

In the case of the second-order model we assume $\lambda_{1,2} = -7.8224 \pm 7.8224j$, $h = 1.5$ and $m = 5$. Matrix R_1 has been chosen equal to

$$R_1 = \begin{bmatrix} 0.566 & 0.0617 \\ 0.0617 & 0.0079 \end{bmatrix}.$$

Matrices Q_p, $p = 1, \ldots, 5$, and R_p, $p = 2, \ldots, 5$, have been determined following the same procedure as in the fourth-order model.

— For the eMPC we considered the same weighting matrix on the states (Q) as in the OGS case. The weight on the input is taken equal to the weight on the input for the OGS case divided by $\rho_{\max}$, i.e., $R_{\text{eMPC}} = R/\rho_{\max}$. This guarantees for both approaches the same level of optimality.

6.1 Some remarks on eMPC

In this section we highlight some problems we encountered when applying the eMPC to the fourth-order model. Let us first observe that in order to reduce the run times we determined the partition of the state space for the fourth-order suspension model considering: $X = \{x \in \mathbb{R}^4 \mid |x_i| \leq 1,\ i = 1, \ldots, 4\}$.

In order to clarify which kind of problems we get into, we reported in Fig. 2 some of the resulting partitions, where a cut at $x_3 = x_4 = 0$ is done. The results relative to the FTOC case with `probStruct.Tconstraint=0` are shown in Fig. 2.a and Fig. 2.b: increasing the prediction horizon N from 10 to 15 the controlled set converges towards the maximum controllable set from the outside inwards. As expected the partition in Fig.2.a cover a larger set than the partition in Fig. 2.b.

The partitions for the FTOC employing `probStruct.Tconstraint=1` are illustrated in Fig. 2.c and Fig. 2.d for $N = 10$ and $N = 15$, respectively. As mentioned above, by increasing the prediction horizon N the controllable set should converge to the maximum controllable set from the inside outwards. Clearly, this is not occurring in this case because parts of the state space that have been covered by the partition with $N = 10$ are not covered by the partition obtained with $N = 15$. Thus, we conclude that some numerical error should have occurred: it is obviously not possible that a state is controllable under a given prediction horizon, but does not maintain this property after increasing the latter.

In the case of the ITOC the unfeasability of the result is even more evident as illustrated in Fig. 3. Only a subset of the state space that was identified to be controllable (see Fig. 2.c) is covered by the ITOC partition: hence a suitable control law exists only in this restricted subset.

These results point out that some of numerical routines of the toolbox MPT [20] are not numerically stable and require to be handled with care. This problem, however, is not addressed in this paper.

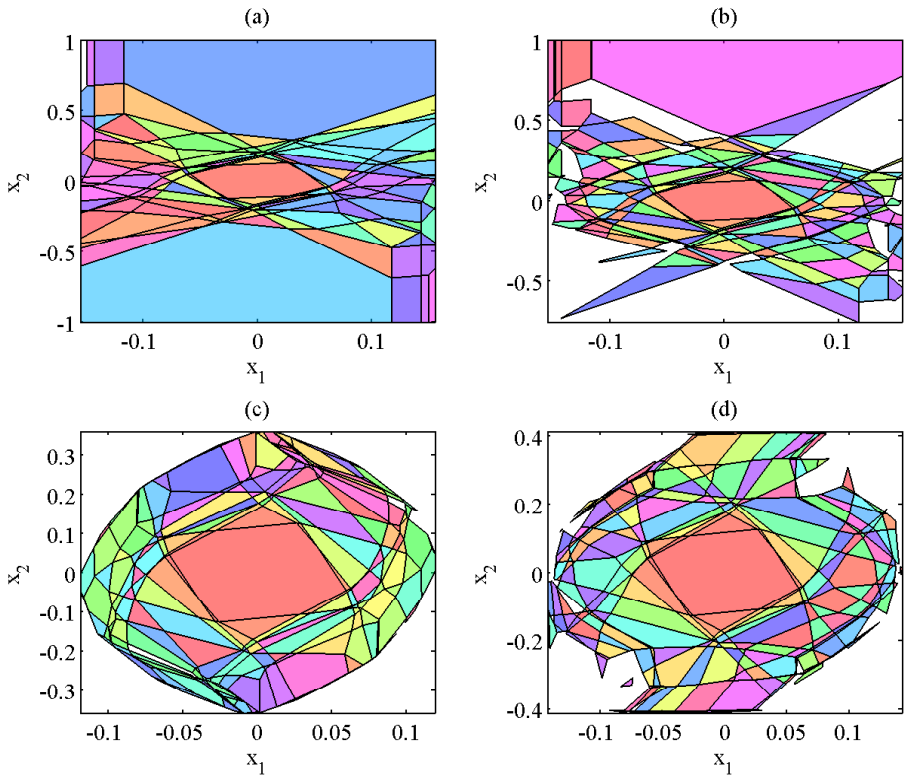

Figure 2: The resulting partitions in the fourth-order case (cut through $x_3 = x_4 = 0$). (a) FTOC, `probstruct:Tconstraint=0`, $N = 10$, 557 regions; (b) FTOC, `probstruct:Tconstraint=0`, $N = 15$, 1038 regions; (c) FTOC , `probstruct:Tconstraint=1`, $N = 10$, 2195 regions; (c) FTOC , `probstruct:Tconstraint=1`, $N = 15$, 3852 regions.

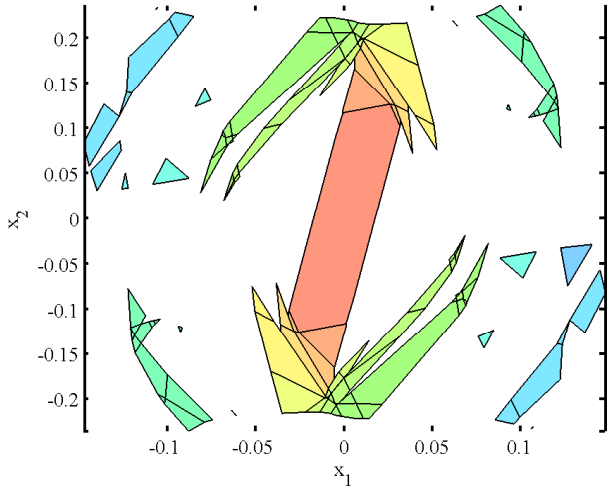

Figure 3: The resulting partitions in the fourth-order case (cut through $x_3 = x_4 = 0$) for the ITOC.

6.2 A comparison among partitions

6.2.1 Second-order model

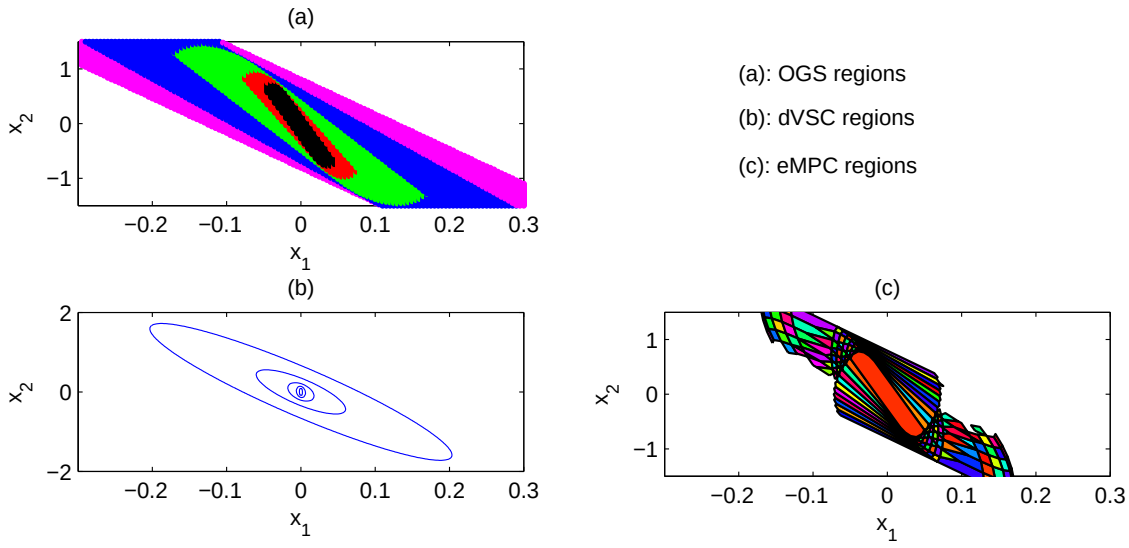

Figure 4: Partition of the state space for the second-order model.

Fig. 4 shows the different state space partitions in the case of the second-order suspension model: the Yoshida regions for the OGS are depicted in Fig. 4.a; Fig. 4.b and Fig. 4.c illustrate the regions resulting from dVSC and eMPC, respectively.

Note that to limit the run times of the computation of the polytopic regions employing eMPC we considered the following bounded polyhedron for the second-order suspension model: $X = \{x \in \mathbb{R}^2 \mid |x_i| \leq 1,\ i = 1, 2\}$. Furthermore, we considered the FTOC with a prediction horizon $N = 10$ and we set `probStruct.Tconstraint=1` to obtain a controller that guarantees closed loop stability and constraint satisfaction for all times.

By looking at Fig. 4 we realize that all procedures provide regions that are large enough to cover the state space region of interest for the considered application. Moreover, the OGS regions are nested, thus we can use them to design a controller. Finally, we observe that the eMPC regions are constrained in the x_2-direction by the assumptions we made in order to reduce the run time (i.e., $x \in X$), but also in the x_1-direction they are smaller than the OGS regions.

6.2.2 Fourth-order model

Fig. 5 depicts a cut through $x_3 = x_4 = 0$ of the partitions obtained with the fourth-order model resulting from the OGS and the eMPC. Here the difference on the size of two state space partitions is even more evident.

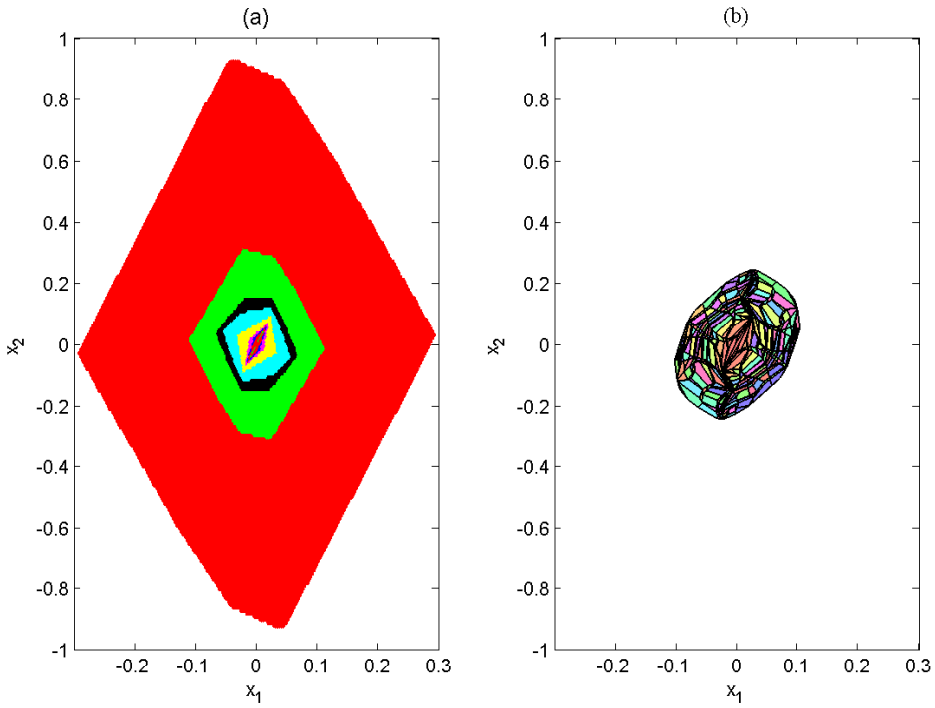

Figure 5: A cut at $x_3 = x_4 = 0$ of the regions obtained for the fourth-order model: (a) OGS (b) eMPC.

Fig. 6 shows a cut thought $x_3 = x_4 = 0$ of the dVSC regions. Comparing this result with those in Fig. 5 it is easy to conclude that the size of the state space partitions obtained using dVSC is intermediate between that of the regions obtained using OGS and that obtained using eMPC.

In any case, even the eMPC cover the portion of the state space that is of interest in practical cases.

Let us also observe that in the eMPC case the size of the covered state space is related to different issues, namely, the constraints on the states ($x \in X$) we introduce to implement the procedure, the options we choose (see the discussion above relative to the setting of parameters in the MPT toolbox), and, in the case of FTOC, the prediction horizon N.

We finally remark that the number of regions obtained using eMPC is significantly higher than the number of regions obtained with the other controllers and their computation is much more burdensome.

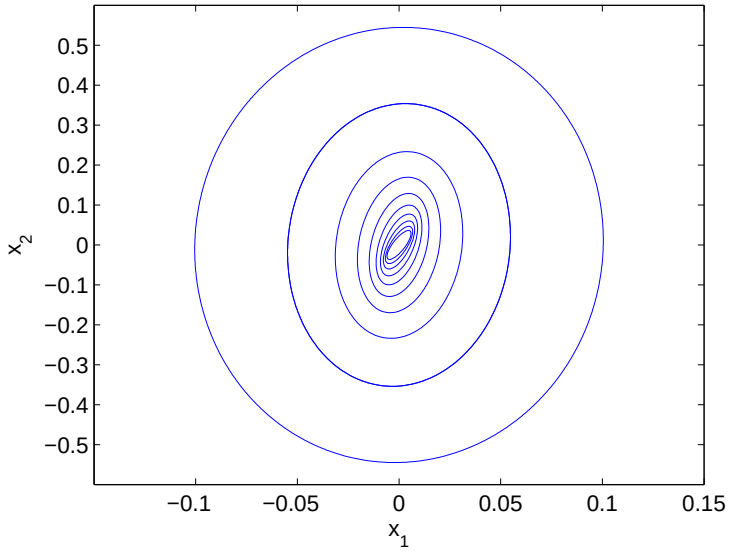

Figure 6: A cut at $x_3 = x_4 = 0$ of the regions obtained for the fourth-order model using dVSC.

6.3 The control performance

6.3.1 Second-order model

In the case of active suspensions we only present the results of numerical simulations carried out on the second-order model, because in such a case all the considered techniques provide state space partitions that are large enough to deal with realistic cases.

We computed the system's evolution for the initial state $x_0 = [0.01\ 0.1]^T$. The simulation results are summarized in Fig. 7. We can observe that the OGS and eMPC controllers determine practically the same system evolution. The dVSC controller provides comparable results in terms of sprung mass position, but with a lower sprung mass velocity.

Finally, in the right bottom graph of Fig. 7 we have pointed out the variation of the index denoting the current region of the state space in the OGS case and in the dVSC case. Here 1 denotes the largest region and 5 the smallest one.

6.3.2 Fourth-order model

In this section we compare the simulation results for the fourth-order suspension model.

Assume that the initial state is $x_0 = [0.015\ 0.1\ 0\ 0]^T$.

Fig. 8 shows the evolution of the semiactive suspension system compared to that of the active suspension in the OGS and in the eMPC case. Note that in the two top figures the two contin-

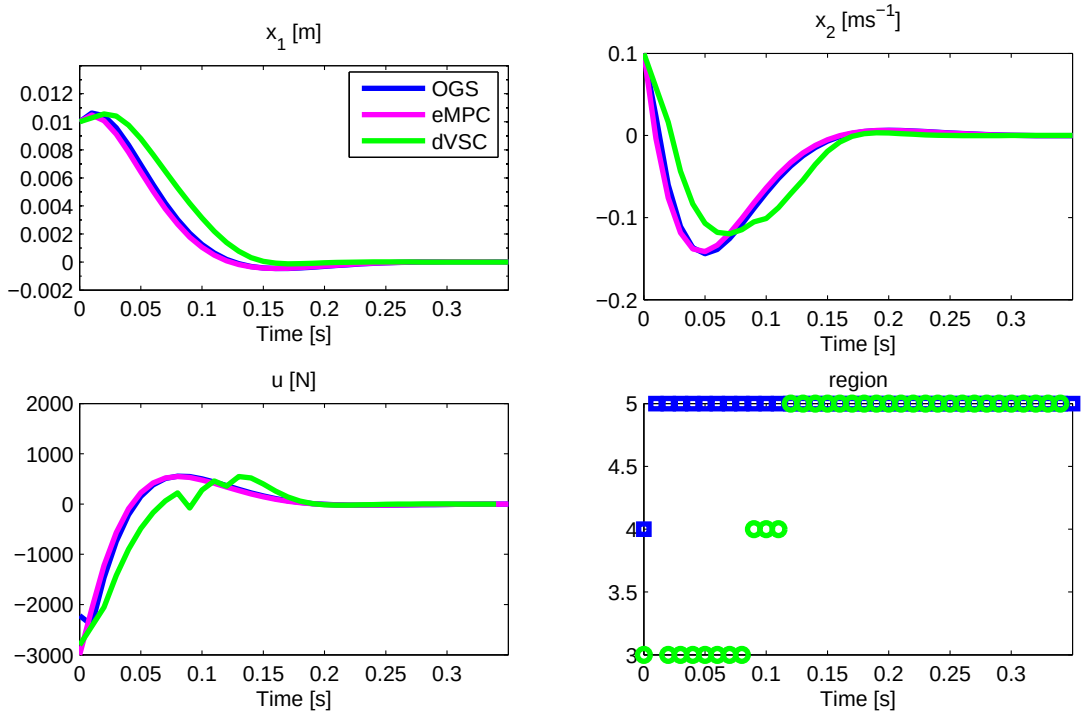

Figure 7: Active suspension and initial state $x_0 = [0.01\ 0.1]^T$. Top-left: sprung mass position x_1. Top-right: sprung mass velocity x_2. Bottom-left: control force u. Bottom-right: index denoting the current region.

uous lines (OGS active and eMPC active) practically coincide, and the two dotted lines (OGS semiactive and eMPC semiactive) also practically coincide.

Again we can conclude that the OGS and the eMPC performances are very similar, and the states at each time instant only differ by an order of magnitude of $|x_{i,\mathrm{OGS}} - x_{i,\mathrm{eMPC}}| \approx 10^{-10}$.

In the bottom left of Fig. 8 we have reported the evolution of the target control laws computed with the OGS and the eMPC, and the control laws that are "really" applied to the system by the semiactive suspension when appropriately adjusting the damping coefficient f (whose variation is shown in the bottom right of Fig. 8). Note that the values of f are undistinguishable in the two cases.

Even better performances are obtained with the dVSC controller. The numerical simulations are reported in Fig. 9. Note that to better compare the performances of the dVSC controller with the previous ones, in the same figure we have reported again the results obtained using eMPC.

This figure enables us to conclude that in the fourth order case the dVSC approach provides the best performances in terms of sprung mass velocity, while comparable results are obtained in terms of sprung mass position.

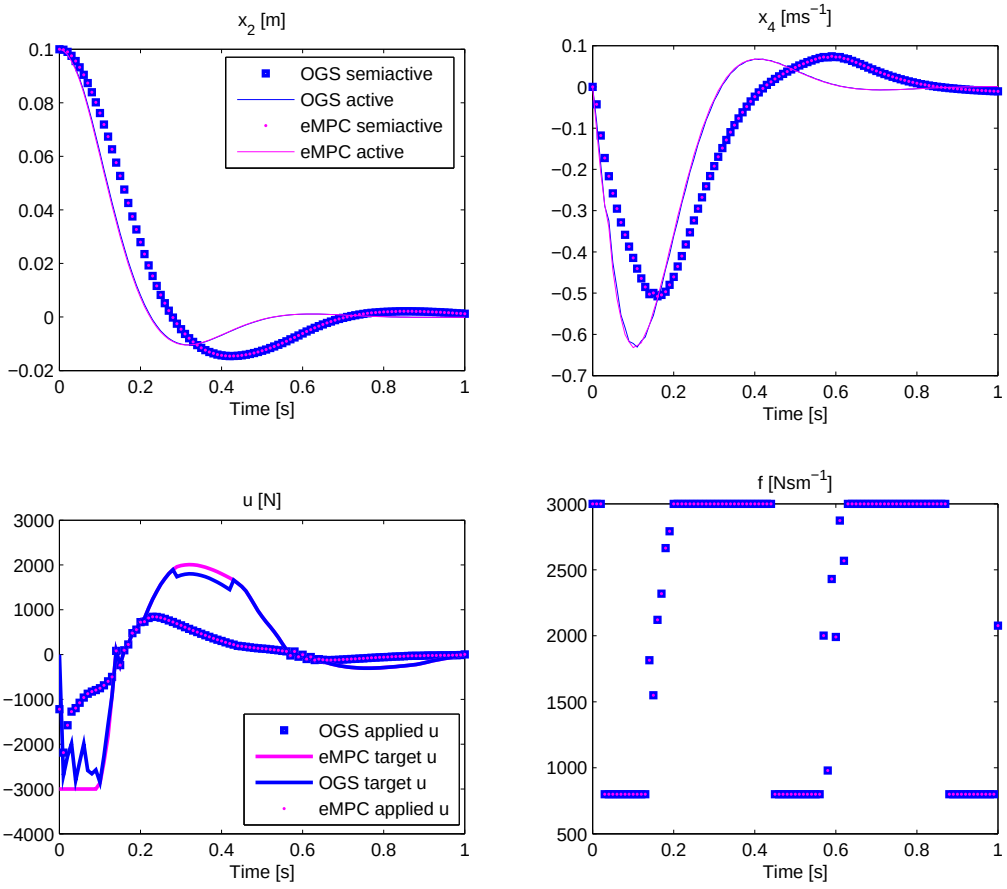

Figure 8: Semiactive suspension with $x_0 = [0.015\ 0.1\ 0\ 0]^T$ using eMPC and OGS. Top-left: sprung mass position x_2. Top-right: sprung mass velocity x_4. Bottom-left: control force u. Bottom-right: value of f in the semiactive suspensions.

7 Conclusions

In this paper we considered three different design techniques, namely *optimal gain switching*, *discontinuous VSC* and *explicit MPC*. All these approaches are based on the computation of an off-line partition of the state space, and guarantee the closed-loop stability and the satisfaction of bounds on the input magnitude. To each convex region a linear or an affine control law is associated, and the on-line phase of the approaches simply consists in selecting the current region. A detailed comparison among these techniques, when applied to the design of semiactive suspension systems, is provided, both in terms of magnitude of the resulting state space partitions, and in terms of the system behaviour. As a result, in this application the three considered approaches provided similar results in terms of performances. However, the computational complexity of the eMPC is surely higher with respect to OGS and dVSC.

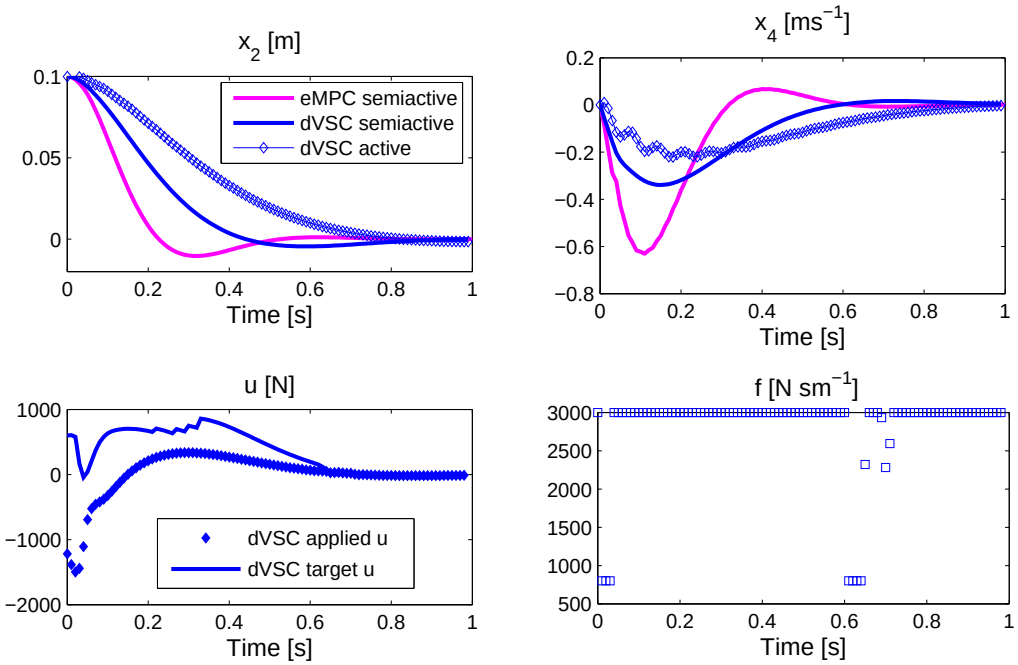

Figure 9: Semiactive suspension with $x_0 = [0.015\ 0.1\ 0\ 0]^T$ using eMPC and dVSC. Top-left: sprung mass position x_2. Top-right: sprung mass velocity x_4. Bottom-left: control force u. Bottom-right: value of f in the semiactive suspensions.

As a limitation of the dVSC we point out the difficulty in determining appropriate values of the design parameters.

Acknowledgments

We would like to thank Michal Kvasnica for his prompt and very helpful support concerning the use of the MPT toolbox.

We also would like to thank an anonymous referee for his/her help in determining appropriate values of the design parameters for the dVSC controller.

References

[1] J. Adamy. Strukturvariable Regelungen mittels impliziter Ljapunov-Funktionen. *Ph.D dissertation, University of Dortmund, Germany*, 1991.

[2] J. Adamy and A. Flemming. Soft variable-structure controls: a survey. *Automatica*, 40:1821–1844, 2004.

[3] A. Bemporad, M. Morari, V. Dua, and E.N. Pistikopoulos. The explicit linear quadratic regulator for constrained systems. *Automatica*, 38:3–20, 2002.

[4] A. Bemporad, A.R. Teel, and L. Zaccarian. Anti-windup synthesis via sampled-data piecewise affine optimal control. *Automatica*, 40(4):549–562, 2004.

[5] A. Bemporad, F.D. Torrisi, and M. Morari. Performance analysis of piecewise linear systems and model predictive control systems. Sydney, Australia, December 2000.

[6] M.J.L. Boada, B.L. Boada, B. Munoz, and V. Diaz. Neural control for a semi-active suspension of a half-vehicle model. *Int. J. of Vehicle Autonomous Systems*, 3(2/3/4), 2005.

[7] F. Borrelli. Discrete time constrained optimal control. *Ph.D dissertation, ETH Zurich*, 2002.

[8] M. Canale, M. Milanese, and C. Novara. Semi-active suspension control using "fast" model-predictive techniques. *IEEE Trans. on Control Systems Technology*, 14(6):1034–1046, 2006.

[9] K.C. Cheok, N.K. Loh, H.D. McGree, and T.F. Petit. Optimal model following suspension with microcomputerized damping. *IEEE Trans. on Industrial Electronics*, 32(4), 1985.

[10] N. Giorgetti, A. Bemporad, H.E. Tseng, and D. Hrovat. Hybrid model predictive control application towards optimal semi-active suspension. *Int. J. of Control*, 79(5):521–533, 2006.

[11] A. Giua, M. Melas, C. Seatzu, and G. Usai. Design of a predictive semiactive suspension system. *Vehicle System Dynamics*, 41(4):277–300, 2004.

[12] A. Giua, C. Seatzu, and G. Usai. Semiactive suspension design with an optimal gain switching target. *Vehicle Systems Dynamics*, 31:213–232, 1999.

[13] A. Hac. Suspension optimisation of a 2-dof vehicle model using a stochastic optimal control technique. *Journal of Sound and Vibration*, 100(3):343–357, 1985.

[14] D. Hrovat. Survey of advanced suspension developments and related optimal control applications. *Automatica*, 33(10):1781–1817, 1997.

[15] N. Jalili. A comparative study and analysis of semi-active vibration-control systems. *J. of Vibration and Acoustics*, 124(4):593–650, 2002.

[16] M.A. Karkoub and M. Zribi. Active/semi-active suspension control using magnetorheological actuators. *Int. J. of Systems Science*, 37(1):35–44, 2006.

[17] H. Kiendl and G. Schneider. Synthese nichtlinearer Regler für die Regelstrecke $const/s^2$ aufgrund ineinander geschalchtelter abgeschlossener Gebiete beschränkter Stellgrösse. *Regelungstechnik und Prozess-Datenverarbeitung*, 20(7), 1972.

[18] M.V. Kothare and M. Morari. Multiplier theory for stability analysis of anti-windup control systems. *Automatica*, 35:917–918, 1999.

[19] E.J. Krasnicki. Comparison of analytical and experimental results for a semi-active vibration isolator. *The Shock and Vibration Bulletin*, pages 69–76, 1980.

[20] M. Kvasnica, P. Grieder, and M. Baotic. Multi-parametric toolbox (mpt). `http://control.ee.ethz.ch/ mpt/`, 2004.

[21] J. Lu and M. DePoyster. Multiobjective optimal suspension control to achieve integrated ride and handling performance. *IEEE Trans. on Control Systems Technology*, 10(6):807–821, 2006.

[22] K. Ogata. Discrete-time control systems. *Prentice Hall International Editions*, 1972.

[23] C. Poussot-Vassal, O. Sename, L. Dugard, R. Ramirez-Mendoza, and L. Flores. Optimal skyhook control for semiactive suspensions. In *4th IFAC Sym. on Mechatronics Systems*, Heidelberg, Germany, 2006.

[24] A.R. Teel, L. Zaccarian, and J.J. Marcinkowski. An anti-windup strategy for active vibration isolation systems. *Control Engineering Practice*, 14(1):17–27, 2006.

[25] A.G. Thompson. An active suspension with optimal linear state feedback. *Vehicle System Dynamics*, 5:187–203, 1976.

[26] W.M. Wonham and C.D. Johnson. Optimal bang-bang control with quadratic performance index. *ASME Journal of Basic Engineering*, 86:107–115, 1964.

[27] K. Yoshida, Y. Nishimura, and Y. Yonezawa. Variable gain feedback control for linear sampled-data systems with bounded control. *Control Theory and Advanced Technology*, 2 (2)(2), 1986.

[28] L. Zaccarian and A.R. Teel. Nonlinear scheduled anti-windup design for linear systems. *IEEE Trans. on Automatic Control*, 49(11):2055–2061, 2004.